

# Topology optimization for lightweight cellular material and structure simultaneously by combining SIMP with BESO<sup>†</sup>

Heting Qiao\*, Shijie Wang, Tiejun Zhao and Henan Tang

*School of Mechanical Engineering, Shenyang University of Technology, Shenyang Liaoning, 110870, China*

(Manuscript Received May 13, 2018; Revised September 23, 2018; Accepted October 24, 2018)

## Abstract

This paper presents a hybrid algorithm for topology optimization of lightweight cellular materials and structures simultaneously by combining solid isotropic material with penalization (SIMP) and bi-directional evolutionary structural optimization (BESO). Microstructure of the lightweight cellular material is assumed unique in the structure to make the proposed method feasible. A new sensitivity analysis formula with respect to the discrete variable is derived by a principal submatrix stiffness matrix, by which the material can be effectively removed from or added to cellular. Moreover, the validity of the proposed method is then demonstrated through two numerical examples (a simple supported beam and a cantilever beam), which can be easily applied in a variety of practical situations.

*Keywords:* Lightweight cellular materials; Topology optimization; SIMP; BESO

## 1. Introduction

Lightweight cellular materials have wide applications in aerospace and mechanical engineering for their multi-function, such as advanced mechanical properties, thermal isolation, anti-impact [1]. From a mechanical point of view, the lightweight structure composed of cellular materials can carry high loading at the minimum weight, as shown in Fig. 1. Therefore, we attempt to find a suitable layout of cellular material in the structure and its own optimum topology simultaneously, and topology optimization methods, such as solid isotropic material with penalization (SIMP) and bi-directional evolutionary structural optimization (BESO), become the preferred tools for this problem.

In a pioneering work of topology optimization, Bendsoe and Kikuchi proposed a homogenization method [2] by introducing the cellular material with square hole into design domain. Then, the solid isotropic material with penalization approach (SIMP) method [3] based on a power law function has been largely used to optimize the structural topology. In their work, traditional topology optimization is treated as material distribution within the macro design domain. Moreover, design results based on this continuous model (SIMP) often have intermediate values of density variables between 0 and 1, especially the material topology optimization. In order to obtain absolute black-and-white design, Xie and Steven developed

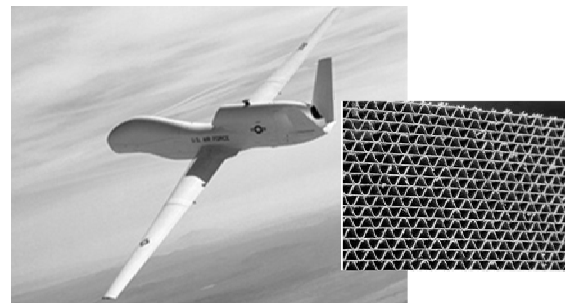


Fig. 1. The application of cellular material in aerospace.

evolutionary structural optimization (ESO) [4] to avoid “grey” elements in the design domain. Recently, some outstanding topology optimization papers [5-9] have presented applications of topology optimization to the sound power flow problem [10], stress constraints problem [11], concrete pipe molding machine [12].

In summary, traditional single-scale structure or material topology optimization problems have attracted much attention. However, with the development of cellular material, a more challenging work is to optimize topology of the structure and material simultaneously. The basic concept of structure-material integrated optimization can trace back to free material optimization (FMO) method [13] by setting the norm or the trace of the elasticity matrix of per point as the design variable. Based on the idea of multiscale topology optimization, Xia [14] develops a design framework for concurrent topology

\*Corresponding author. Tel.: +86 13998381743, Fax.: +86 24 25496271  
E-mail address: qiaoheting@mail.neu.edu.cn

<sup>†</sup>Recommended by Associate Editor Gil Ho Yoon

© KSME & Springer 2019



Fig. 2. The checkerboard pattern of lightweight cellular material.

optimization of material and structure by using FE<sup>2</sup> nonlinearity analysis method. Recently, Coelho [15] extended a multiscale topology optimization model to the bi-material composite laminate.

Furthermore, the optimum microstructure of material based on FMO method varies from point to point, which will make the design results difficult to manufacture in the practical engineering. In order to solve this problem, Cheng [16] presents porous anisotropic material with penalization (PAMP) to concurrent topology optimization of structure and material by defining only one microstructure of truss-like material in design domain. Based on the idea of PAMP [16], Sivapuram [17] propose an approach using the level-set method at both scales to solve the minimizing compliance and compliant mechanism problems; Chen [18] presents the new moving isosurface threshold formulation and algorithm to solve checkerboard pattern and grey problem in concurrent design; Long [19] develop a ICM (independent, continuous and mapping) based model to minimize total mass under multiple constraints. Some recent successful applications of concurrent topology optimization often focus on the extension to multiple porous materials [20, 21].

Although some successful examples of concurrent topology optimization of structure and material were reported, most of the designs were based on the conventional mathematical programming method. Unfortunately, there are still some problems due to its complexity, such as checkerboard pattern and grey problem, as shown in Fig. 2 [16]. In this paper, considering mechanical performance, we continue concurrent design the topology of structure and cellular material by emphasizing an identical microstructure in macro-scale. The structural layout at macro-scale and topology of cellular material at micro-scale are optimized simultaneously to achieve minimum compliance. To suppress the checkerboard pattern and grey problem in topology optimization (Fig. 2 [16]), the authors of this paper propose a method to solve this problem by combining SIMP and BESO. Thus, SIMP model are applied on the elements of structure, and the discrete form are applied on the elements of cellular material. Because two independent volume constraint functions are respectively applied to continuous and discrete design variables, the optimization model with hybrid continuous /discrete design variables is solved by combining two methods MMA [22] and BESO [4, 23]. In this way, optimum structural topology with optimum microstructure of lightweight cellular material can be obtained effectively.

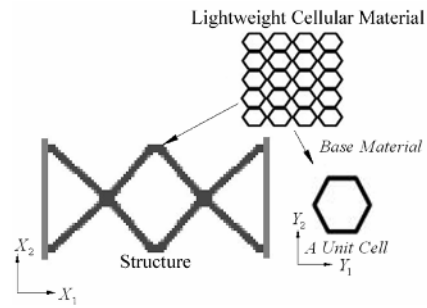


Fig. 3. Lightweight structure with cellular material.

The organization of the present paper is as follows. A continuous /discrete hybrid optimization model is built in Sec. 2. Sec. 3 provides a more accurate sensitivity analysis formula with respect to the discrete variable. Sec. 4 describes the combined algorithm for concurrent topological optimization of the structure and cellular. Sec. 5 outlines two numerical examples in order to validate the presented method. Finally, we conclude in Sec. 6 with a discussion.

**2. Problem statement and the mechanical model**

In this paper, we are trying to obtain optimum topology in two-scale [24] with an identical microstructure of cellular material, as shown in Fig. 3.

This problem can be looked as a two-scale layout design, in which the material distribution in two-scale will be optimized by topology optimization method. According to the literature, clear structural topology based SIMP can be easily obtained by using filter technology [25], but optimum microstructure of material often encounter checkerboard pattern and grey problem. Therefore, two types design variables are independently defined, the first one is the macro density  $\rho(\Omega)$  in structural design domain, ranging from 0 to 1; the other one is micro density  $h(\Psi)$  in a unit cell, which can be only taken as two values 0 and 1 indicating the void and solid element, and middle density elements between 0 and 1 will not appear in the unit cell. The hybrid continuous /discrete optimization model of linearly elastic structures can be written as

$$\begin{aligned}
 \text{Find: } & \mathbf{X} = \{\rho_1, \rho_2, \dots, \rho_M, h_1, h_2, \dots, h_N\}^T \\
 \text{min: } & C = \mathbf{F}^T \mathbf{U} \\
 \text{s.t.: } & \varphi = \frac{\int \rho d\Omega}{|\Omega|} \leq \bar{\varphi} \\
 & \xi = \frac{\int h d\Psi}{|\Psi|} \leq \bar{\xi} \\
 & 0 \leq \rho_i \leq 1 \quad i = 1, 2, \dots, M \\
 & h_j \in \{0, 1\} \quad j = 1, 2, \dots, N
 \end{aligned} \tag{1}$$

where the objective function C is the structural compliance.  $\Omega$  which is the macro design domain represent the structure,

and  $\Psi$  which is the micro design domain represent the cellular material.  $M$  is the element number in the structure design domain  $\Omega$  and  $N$  is the element number in the unit cell  $\Psi$ .  $F$  and  $U$  is the structural global displacement and force vector respectively. Two independent volume constraint functions are respectively applied to continuous and discrete design variables. Constraint I is applied on the total volume of lightweight cellular material in the macro design domain by an upper bound  $\bar{\zeta}$ , similar as single-scaled structural topology optimization. Constraint II is applied on the total volume of base material in the unit cell by an upper bound  $\bar{\xi}$ , which should be between 0.2 and 0.6 according to practical fabrication techniques.

In order to compute the structural compliance, the first step is solving the following finite element equation to obtain the structural deformation.

$$\begin{aligned} KU &= F \\ K &= \int_{\Omega} B^T D^M B d\Omega. \end{aligned} \tag{2}$$

Here,  $K$  represents the global stiffness matrix of the structure.  $U$  and  $F$  denote the global displacement and force vector, and  $B$  is the strain/displacement matrix. Base on the SIMP method, the modulus matrix  $D^M$  in macro design domain is defined by a power law of the homogenized elastic matrix  $D^H$  of the lightweight cellular material, as follow

$$D^M = \rho^\alpha D^H \tag{3}$$

where  $\alpha$  denotes the exponent of penalization. The homogenized elastic matrix  $D^H$  can be looked as a crucial connection between structure and lightweight cellular material, and can be defined by the classical homogenization equation

$$D^H = \frac{1}{|\Psi|} \int_{\Psi} (D^0 - D^0 B \Phi) d\Psi \tag{4}$$

where  $D^0$  is the elastic matrix of solid material in the base cell  $\Psi$ . The characteristic displacements  $\Phi$  are the periodic solutions of

$$\begin{aligned} K^H \Phi &= P \\ P &= \int_{\Psi} B^T D^0 d\Psi \end{aligned} \tag{5}$$

where  $K^H$  denote the globe stiffness matrix of the base cell  $\Psi$ .

### 3. Sensitivity analysis of the discrete variable

In the collaborative optimization problem (1), the lightweight cellular material is described by the base cell  $\Psi$ . Moreover, the density of each element  $h_e$  in the base cell will be either 1 or 0, and the optimal topology of the lightweight cellular material can be obtained by BESO method.

At present, the sensitivity analysis with respect to discrete

variables is adopted to determine which element the material should be removed from or added in. In order to avoid the inaccurate sensitivity analysis, especially when a void element is changed to a solid element, a new sensitivity analysis formula is derived based on binary discrete method [4, 23].

Thus, the change of the effective elastic matrix  $D^H$  in Eq. (4) can be formulated by using first-order Taylor expansion

$$\Delta D^H = \frac{1}{|\Psi|} \int_{\Psi} \left( (\mp D^0) - (\mp D^0) B \Phi - D^0 B (\delta \Phi) \right) d\Psi. \tag{6}$$

Here, the sign “-” represent the material removal, and the sign “+” represent the material addition, as following formulas. And  $\delta \Phi$  is the increment of the characteristic displacement  $\Phi$  in Eq. (5), and  $\delta \Phi$  satisfies

$$\begin{aligned} (K^H + \Delta K^H) \delta \Phi &= \Delta P - \Delta K^H \Phi \\ \Delta P &= \int_{\Psi} B^T (\mp D^0) d\Psi. \end{aligned} \tag{7}$$

When material removal or addition is allowed in the base cell  $\Psi$ ,  $\Delta K^H$  which is the change of  $K^H$  can be computed as following

$$\begin{aligned} \Delta K^H &= \mp K_e^H \\ K_e^H &= \int_{\Psi_e} (B^T D^0 B) d\Psi_e. \end{aligned} \tag{8}$$

Here,  $K_e^H$  is the element stiffness matrix of the base cell.

Based on the traditional method, the above Eq. (7) can be solved approximately by

$$\delta \Phi \approx (K^H)^{-1} (\Delta P - \Delta K^H \Phi). \tag{9}$$

In this paper, a principal submatrix stiffness matrix [23] is introduced into the sensitivity analysis of the homogenized elastic matrix, when the material is removed from or added to the unit cell, which can provide good estimation of change of the homogenized elastic matrix with respect to the discrete variable. Thus,  $\delta \Phi$  can be expressed formally as

$$\delta \Phi = (K^H)^{-1} K_{NL}^H (\Delta P - \Delta K^H \Phi) \tag{10}$$

where  $K_{NL}^H$  stands for the change of  $K^H$  with higher precision

$$K_{NL}^H = K_{sub}^H (K_{sub}^H + K_v^H)^{-1}. \tag{11}$$

Here,  $K_{sub}^H$  is the principal submatrix stiffness matrix of  $K^H$ .  $K_{sub}^H$  must include the element  $e$ , where material removal or addition will occur, as shown in the Fig. 4.  $K_v^H$  is a new matrix, and can be written as

$$K_v^H = \begin{cases} 0, & (\Delta K^H = -K_e^H, \text{material removal}) \\ \Delta K^H, & (\Delta K^H = K_e^H, \text{material addition}). \end{cases} \tag{12}$$

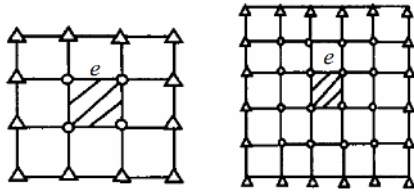


Fig. 4. Substructure of  $K_{sub}^H$ .

In the Fig. 4,  $\Delta$  present the fixed node in the substructure.

Substituting Eq. (10) into Eq. (6), the sensitivity Eq. (6) can be rewritten formally

$$\Delta D^H = \frac{1}{|\Psi|} \left( \Delta \bar{D}^0 - \Delta P^T K_{NL}^H \Phi - \Phi^T K_{NL}^H \Delta P + \Phi^T K_{NL}^H \Delta K^H \Phi \right)$$

$$\Delta \bar{D}^0 = \int_{\Psi} \mp D^0 d\Psi. \tag{13}$$

When a solid element is changed to a void element,  $K_{NL} = I$ , Eq. (13) can be written as

$$\Delta D^H = \frac{1}{|\Psi|} \left( \Delta \bar{D}^0 - \Delta P^T \Phi - \Phi^T \Delta P + \Phi^T \Delta K^H \Phi \right). \tag{14}$$

Substituting Eqs. (7) and (8) into Eq. (14), Eq. (14) can be furtherly rewrote as

$$\Delta D^H = \frac{1}{|\Psi|} \int_{\Psi} \left( -D^0 - (-D^0) B \Phi - \Phi^T B^T (-D^0) + \Phi^T B^T (-D^0) B \Phi \right) d\Psi$$

$$= \frac{1}{|\Psi|} \int_{\Psi} (I - B \Phi)^T (-D^0) (I - B \Phi) d\Psi. \tag{15}$$

Obviously, above Eq. (15) is definitely same to the formula in the Refs. [19, 21] (Eq. (14a) in the Ref. [19], Eq. (20) in the Ref. [21]), as following

$$\frac{\partial D^H}{\partial x} = \frac{1}{|\Psi|} \int_{\Psi} (I - B \Phi)^T \frac{\partial D}{\partial x} (I - B \Phi) d\Psi. \tag{16}$$

Therefore, when the material is removed from a solid element, the sensitivity analysis of the homogenized elastic matrix can be calculated by Eq. (15); when the material is add to a void element, the sensitivity analysis of the homogenized elastic matrix can be calculated by Eq. (13).

Moreover, the sensitivity of structural compliance with respect to the discrete variable  $h(\Psi)$  can be computed as

$$\Delta C = -U^T \Delta K U$$

$$\Delta K = \int_{\Omega} B^T \Delta D^H B d\Omega. \tag{17}$$

#### 4. Combined solving algorithm

In this section, we will present a combined algorithm to iterative solve the hybrid optimization model, which can be

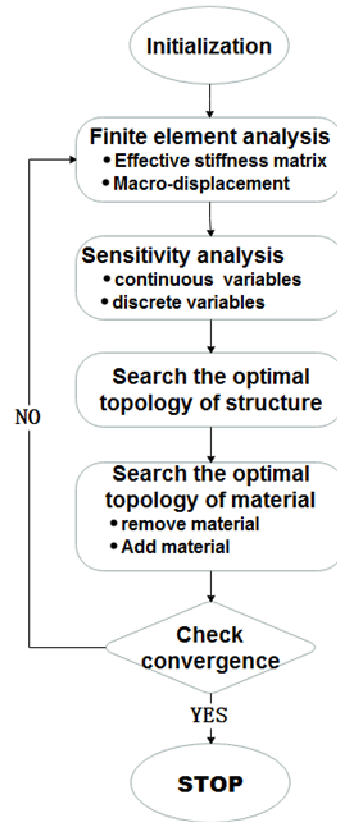


Fig. 5. Flow chart of combined solving algorithm.

easily achieved by using the secondary development in ANSYS. Moreover, compared to the previous method (PAMP, level set) [16, 17], the clear topology of cellular material based on the proposed method can be easier obtained by the sorting program. The combined solving algorithm is summarized below, as shown in Fig. 5.

**Step 1.** Initialization: prescribe the maximum volume of material removal  $\gamma$  and addition  $\eta$  in each design iteration, which usually are set by 5 % and 3 % of the unit cell;

**Step 2.** Finite element analysis: compute the effective stiffness tensor, and obtain the displacement vector of the current structure;

**Step 3.** Sensitivity analyses:

① For continuous design variables, obtain the sensitivity of the structural compliance by;

$$\frac{\partial C}{\partial \rho_e} = - \frac{\alpha U_e^T K_e U_e}{\rho_e}. \tag{18}$$

In order to avoid checkerboard and grey problem, the sensitivity filter method [25] (Eq. (16) in the Ref. [25]) is adopted to continuous design variables as following

$$\widetilde{\frac{\partial C}{\partial \rho_e}} = \frac{\sum_{i \in N_e} \omega(\rho_i) \rho_i \frac{\partial C}{\partial \rho_i}}{\rho_e \sum_{i \in N_e} \omega(\rho_i)}. \tag{19}$$

② For discrete design variables, compute the sensitivity of the structural compliance for the solid and void element by Eqs. (11)-(15);

**Step 4.** Search the optimal topology of structure by MMA: Method of moving asymptote is employed to search the optimal topology of structure, and only continuous design variables are updated in this step.

**Step 5.** Search the optimal topology of the lightweight cellular material by BESO: After compute the total material volume  $\xi$  in the unit cell, give values to  $\gamma$  and  $\eta$  as following

$$\begin{cases} \text{if } \xi > \bar{\xi} \text{ and } \gamma > \eta & null \\ \text{if } \xi > \bar{\xi} \text{ and } \gamma \leq \eta & \gamma = 1.05\eta \\ \text{if } \xi \approx \bar{\xi} & \gamma = \eta \\ \text{if } \xi < \bar{\xi} \text{ and } \gamma < \eta & null \\ \text{if } \xi < \bar{\xi} \text{ and } \gamma \geq \eta & \gamma = 0.95\eta \end{cases} \quad (20)$$

① Remove material: Sort all the solid elements in the cell based on the sensitivity from small to large. Then, update top ranking solid elements to void elements, when their volume is equal to the required material removal amount  $\gamma$ .

② Add material: Sort all the void elements in the cell based on the sensitivity from small to large (absolute value from large to small). Then, update top ranking void elements to solid elements, when their volume is equal to the required material addition amount  $\eta$ .

**Step 6.** Convergence checking: convergence is examined by the following criterion

$$\begin{cases} \frac{|C_k - C_{k-1}|}{|C_k|} \leq \Delta \\ \xi \approx \bar{\xi} \end{cases} \quad (21)$$

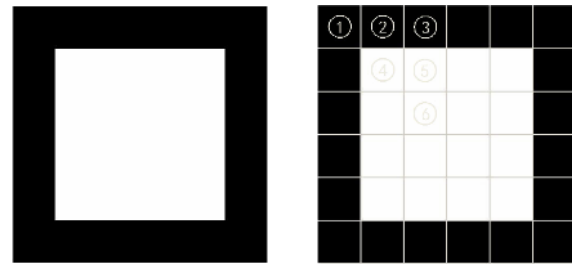
where  $k$  is the current iteration, and  $\Delta$  is a specified small value( $10^{-8}$ ). If  $\frac{|C_k - C_{k-1}|}{|C_k|} \leq \Delta$  and  $\xi \approx \bar{\xi}$  are satisfied simultaneously, stop; else, go back to step 2.

## 5. Numerical examples

### 5.1 Sensitivity test

In this example, the validity of sensitivity analysis Eqs. (13)-(15) is verified by a hollow square unit cell, as shown in Fig. 6.

The square unit cell is divided into  $6 \times 6$  rectangular elements. According to symmetry of the unit cell, only 6 elements need to be observed, as shown in Fig. 6. The Young's modulus of base material is  $E = 2 \times 10^{11}$ , and Poisson's ratio  $\mu$  is 0.3. For comparison, the sensitivity of homogenized elastic matrix with respect to each element (solid and void) is calculated by proposed Eqs. (13)-(15) and traditional formula. In order to evaluate error of the sensitivity obtained by differ-



A hollow square unit cell      Finite element model  
Fig. 6. A hollow square unit cell and its finite element model.

ent method, the result generated by difference method is dealt as standard. The difference formula can be written as

$$\Delta \bar{D}^H = {}^e \bar{D}^H - D^H \quad (22)$$

where  $D^H$  is the current homogenized elastic matrix of unit cell.  ${}^e \bar{D}^H$  is the homogenized elastic matrix of next iteration, when material is removed from or add to the element  $e$ . Moreover, the error estimation formula can be expressed

$$error = \max \left( \left| \frac{\Delta D_{ij}^H - \Delta \bar{D}_{ij}^H}{\Delta \bar{D}_{ij}^H} \right| \right) \quad i, j = 1, 2, 3. \quad (23)$$

Based on the traditional formula and proposed formula, sensitivity of homogenized elastic matrix and its error are listed in Tables 1 and 2. It is clear that results obtained by proposed formula are identical with results obtained by traditional formula, when the material is removed from a solid element (1, 2, 3). However, the error by using traditional formula goes to very large even infinity, when the material is added to a void element (4, 5, 6). In order to suppress the inaccuracy of sensitivity with respect to void element, Eq. (13) proposed in this paper estimate precisely the change of homogenized elastic matrix during evolution, and error is less than 20%, as shown in Table 2.

### 5.2 Numerical example I: A validation of the proposed method

The purpose of the benchmark MBB beam is to prove the effectiveness of proposed method. The optimum topologies of structure and cellular material generated by PAMP [16] and the new proposed method are presented for comparison.

In this numerical example, a rectangular domain with a height-to-length ratio  $H/L = 25/50$  is simply supported at the two bottom edges and loaded by a concentrated vertical force, as shown in Fig. 7. For simplicity, only the right half part is set to be structural design domain due to symmetry. The macro design domain is discretized into  $50 \times 25$  four-node elements, and the unit cell is meshed by  $25 \times 25$  four-node elements. The Young's modulus of solid material is  $E = 2.1 \times 10^5$ , and Poisson's ratio  $\mu$  is assumed to be 0.3. The total volume of the lightweight cellular material in the structure is constrained by

Table 1. Sensitivity of homogenized elastic matrix.

No	$\Delta \mathbf{D}^H$ (traditional formula, $10^9$ )	$\Delta \mathbf{D}^H$ (proposed formula, $10^9$ )	$\Delta \bar{\mathbf{D}}^H$ (difference, $10^9$ )
1	$\begin{bmatrix} -7.73 & 0.62 & 0.55 \\ 0.62 & -7.73 & 0.55 \\ 0.55 & 0.55 & -0.76 \end{bmatrix}$	$\begin{bmatrix} -7.73 & 0.62 & 0.55 \\ 0.62 & -7.73 & 0.55 \\ 0.55 & 0.55 & -0.76 \end{bmatrix}$	$\begin{bmatrix} -7.15 & 0.51 & 0.42 \\ 0.51 & -7.15 & 0.42 \\ 0.42 & 0.42 & -0.72 \end{bmatrix}$
2	$\begin{bmatrix} -19.66 & -2.53 & 4.22 \\ -2.53 & -2.18 & 1.42 \\ 4.22 & 1.42 & -1.57 \end{bmatrix}$	$\begin{bmatrix} -19.66 & -2.53 & 4.22 \\ -2.53 & -2.18 & 1.42 \\ 4.22 & 1.42 & -1.57 \end{bmatrix}$	$\begin{bmatrix} -22.08 & -2.69 & 5.00 \\ -2.69 & -2.29 & 1.36 \\ 5.0 & 1.36 & -1.79 \end{bmatrix}$
3	$\begin{bmatrix} -21.85 & -3.83 & 1.62 \\ -3.83 & -0.57 & -0.04 \\ 1.62 & -0.04 & -1.12 \end{bmatrix}$	$\begin{bmatrix} -21.85 & -3.83 & 1.62 \\ -3.83 & -0.57 & -0.04 \\ 1.62 & -0.04 & -1.12 \end{bmatrix}$	$\begin{bmatrix} -25.02 & -3.01 & 1.77 \\ -3.01 & -0.48 & -0.05 \\ 1.77 & -0.05 & -0.97 \end{bmatrix}$
4	$\begin{bmatrix} 14.49 & 7.38 & -4.84 \\ 7.38 & 14.49 & -4.84 \\ -4.84 & -4.84 & 9.15 \end{bmatrix}$	$\begin{bmatrix} 3.69 & 1.74 & -2.85 \\ 1.74 & 3.69 & -2.85 \\ -2.85 & -2.85 & 2.45 \end{bmatrix}$	$\begin{bmatrix} 3.31 & 1.83 & -2.46 \\ 1.83 & 3.31 & -2.46 \\ -2.46 & -2.46 & 2.61 \end{bmatrix}$
5	$\begin{bmatrix} 11.59 & 6.64 & -1.67 \\ 6.64 & 15.67 & -0.42 \\ -1.67 & -0.42 & 10.09 \end{bmatrix}$	$\begin{bmatrix} 1.58 & 0.08 & -0.21 \\ 0.08 & 0.00 & -0.01 \\ -0.21 & -0.01 & 0.02 \end{bmatrix}$	$\begin{bmatrix} 1.36 & 0.09 & -0.18 \\ 0.09 & 0.00 & -0.01 \\ -0.18 & -0.01 & 0.02 \end{bmatrix}$
6	$\begin{bmatrix} 14.27 & 5.72 & -0.49 \\ 5.72 & 14.27 & -0.49 \\ -0.49 & -0.49 & 7.24 \end{bmatrix}$	$\begin{bmatrix} 0.00 & 0.00 & 0.00 \\ 0.00 & 0.00 & 0.00 \\ 0.00 & 0.00 & 0.00 \end{bmatrix}$	$\begin{bmatrix} 0.00 & 0.00 & 0.00 \\ 0.00 & 0.00 & 0.00 \\ 0.00 & 0.00 & 0.00 \end{bmatrix}$

Table 2. Error of sensitivity analysis.

No	Traditional formula	Proposed formula
1	26 %	26 %
2	16 %	16 %
3	19 %	19 %
4	440 %	16 %
5	223900 %	17 %
6	$\infty$	11 %

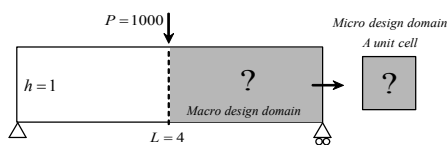


Fig. 7. MBB beam.

$\bar{\zeta} = 0.6$ , and the volume of solid material in the unit cell is limited by  $\bar{\xi} = 0.3$ . The material removal ratio  $\gamma$  and addition ratio  $\eta$  are chosen to be 5 % and 3 %, respectively during the evolution.

The evolution history is shown in Table 1. The material removal in unit cell started with  $\xi = 1.0$  and this value was reduced to  $\xi = 0.3$  during the process. In order to compare the optimum design of SIMP method and the proposed method, SIMP method is used in solving the MBB beam problem under the volume constraint  $\bar{V} = \bar{\zeta} \times \bar{\xi} = 0.6 \times 0.3 = 0.18$ . This is to say, the total volume constraint of solid material in SIMP method and the proposed method are the same, as shown in the column

2 of Table 3. The results in the column 3-4 of Table 3, obtained by the present method, are the final topologies of the structure and material. They are also similar with the results shown Table 4 obtained by Cheng et al. [16]. Therefore, the ability of the proposed method to obtain optimum topologies of structure and material simultaneously is verified by this example. Compared to the method in the Ref. [16], the convergence can be easier obtained by proposed method due to absolute ‘black-and-white’ topology of material, and the proposed method can be easily achieved by traditional topology optimization program. The advantage of the proposed method is shown as following Table 4.

### 5.3 Numerical example II: A discussion of parameters $\bar{\xi}$

In this example, a cantilever beam with geometric parameters  $L = 60$  and  $h = 30$  is fixed on the left edge, and the distributed constant pressure is loaded at the top edge with  $q = 10^6$ , as shown in Fig. 8. Solid material is assumed to have Young’s modulus  $E = 2.1 \times 10^5$  and Poisson’s ratio  $\mu = 0.3$ . The macro design domain is mesh by  $60 \times 30$  four-node elements, and the unit cell of material is discretized by using  $25 \times 25$  four-node elements. To illustrate the influence of the perimeters  $\bar{\zeta}$  and  $\bar{\xi}$ , the optimization problem is solved with fixed the total volume of solid material  $\bar{\zeta} \times \bar{\xi} = 0.12$  and varying perimeter  $\bar{\xi}$ , as shown in Tables 5 and 6.

The cantilever beam problem shown in Fig. 8 is solved for 11 different  $\bar{\xi}$ . The optimum topologies of structure and material generated by proposed method are listed in the Tables

Table 3. Evolution history.




























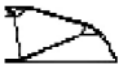




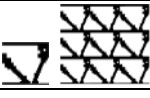
Iteration	Structural topology (SIMP)	Structural topology (proposed mehtod)	Microstructural topology
Initial			
5			
10			
15			
20			
25			
30			
35			
40			









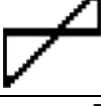

Table 4. Optimal topologies of the structure and material by using different methods: SIMP; the method by Cheng et al. [16]; the present method.

Method	Structural topology	Microstructural topology	Iterations	Structural compliance
SIMP			40	1268
PAMP [16]			60	2234
The present method			40	1752

5 and 6. When the upper bound  $\bar{\xi}$  is set to be 1.0, any material can't be removed from the unit cell. Therefore, the optimum structure topology obtained by the proposed method is definitely same as the optimum topology obtained by SIMP under  $\bar{\xi} = 1.0$ , as show in the top row of Table 6. From the resulting compliances, we see that lower system compliance

can be obtained by increasing  $\bar{\xi}$  in this case, as shown in Fig. 9. In other words, adding material to the unit cell is better than adding material to the structure on this configuration. Moreover, the optimum topology of the cellular material in this example is a triangle cell, which is believed a common configuration in the practical engineering, as shown in Fig. 1.

Table 5. Results of the cantilever beam design.

$\bar{\xi}$	$\bar{\zeta}$	$C(10^3)$	$D'' (10^4)$	Microstructural topology
1.0(SIMP)	0.12	0.481	$\begin{bmatrix} 23.08 & 6.923 & 0 \\ 6.923 & 23.08 & 0 \\ 0 & 0 & 8.077 \end{bmatrix}$	
0.6	0.2	0.775	$\begin{bmatrix} 21.479 & 3.272 & -3.374 \\ 3.272 & 6.097 & -3.336 \\ -3.374 & -3.336 & 3.494 \end{bmatrix}$	
0.55	0.218	0.797	$\begin{bmatrix} 20.302 & 2.530 & -2.537 \\ 2.530 & 2.649 & -2.4847 \\ -2.537 & -2.485 & 2.662 \end{bmatrix}$	
0.50	0.24	0.804	$\begin{bmatrix} 15.872 & 2.480 & -2.547 \\ 2.480 & 4.967 & -2.478 \\ -2.547 & -2.478 & 2.658 \end{bmatrix}$	
0.45	0.267	0.806	$\begin{bmatrix} 11.419 & 3.439 & -3.420 \\ 3.439 & 4.727 & -3.409 \\ -3.420 & -3.409 & 3.551 \end{bmatrix}$	
0.4	0.3	0.817	$\begin{bmatrix} 10.172 & 3.366 & -4.424 \\ 3.366 & 5.575 & -4.360 \\ -4.424 & -4.360 & 5.476 \end{bmatrix}$	
0.35	0.343	0.846	$\begin{bmatrix} 8.853 & 3.318 & -3.354 \\ 3.318 & 4.444 & -3.308 \\ -3.354 & -3.308 & 4.410 \end{bmatrix}$	
0.3	0.4	0.883	$\begin{bmatrix} 12.572 & 2.294 & -2.261 \\ 2.294 & 3.382 & -2.238 \\ -2.261 & -0.238 & 3.332 \end{bmatrix}$	
0.25	0.48	0.974	$\begin{bmatrix} 8.297 & 2.215 & -2.234 \\ 2.215 & 2.291 & -2.209 \\ -2.234 & -0.209 & 2.266 \end{bmatrix}$	
0.2	0.6	1.456	$\begin{bmatrix} 7.043 & 1.172 & -1.174 \\ 1.172 & 2.214 & -1.157 \\ -1.174 & -0.157 & 2.205 \end{bmatrix}$	

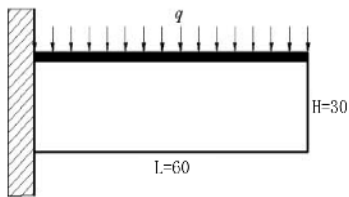


Fig. 8. A cantilever beam subjected to a distributed constant line load.

**6. Conclusions**

The purpose of this research is to optimize the topology of structure and lightweight cellular material simultaneously by a new concurrent design method. Considering mechanical performance and request of actual engineering (only a material microstructure in the structure), the strategy based on the uni-

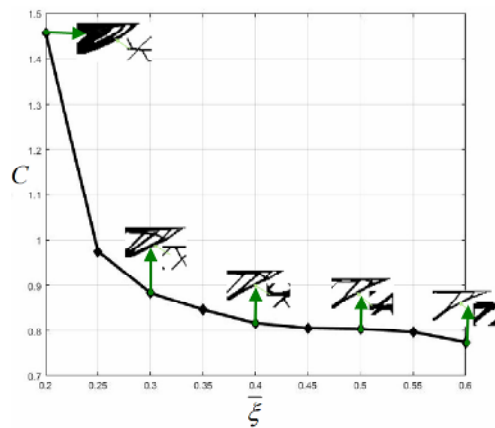
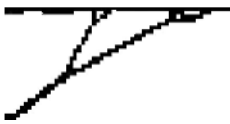


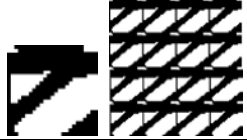



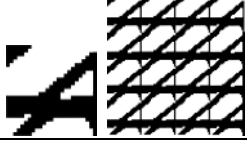

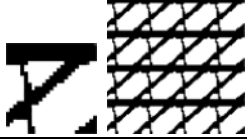

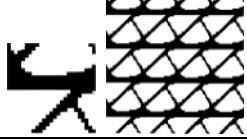

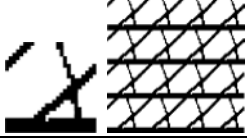

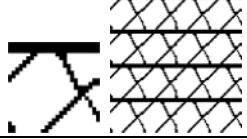

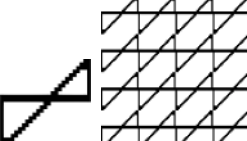

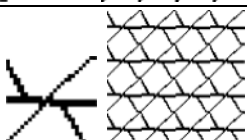


Fig. 9. The optimal structural compliance with the varying  $\bar{\xi}$ .



Table 6. Results of the cantilever beam design.

$\bar{\xi}$	Structural topology	Microstructural topology
1.0 (SIMP)		
0.6		
0.55		
0.50		
0.45		
0.4		
0.35		
0.3		
0.25		
0.2		

formity of material microstructure continue to be used in this paper. The optimization model with hybrid continuous/discrete design variables is formulated for concurrent topology optimization of lightweight cellular materials and structures. A new solving algorithm is proposed by combining

MMA and BESO. The proposed method is applied to a MBB beam and a cantilever beam. From those two common cases, it is concluded that different  $\bar{\xi}$  (the upper bound of volume of solid material in the unit cell) settings will result different optimum topology of both structure and cellular

material, and a triangle cell based material is suitable for the simply supported beam and cantilever beam. Furthermore, compared to PAMP [16], the proposed method shows a better convergence of the optimum topologies of material and structure due to absolute ‘black-and-white’ design of the cellular material.

## Acknowledgments

This work was supported by Research Program supported by National Natural Science Foundation of China (Grant No. 51505298) and Natural Science Foundation of Liaoning Province of China (Grant No. 20170520143), China.

## Nomenclature

$E$	: Young’s modulus
$\mu$	: Poisson’s ratio
$\mathbf{D}^H$	: Homogenized elastic matrix
$\mathbf{K}$	: Global stiffness matrix
$\mathbf{U}$	: Global displacement vector
$\mathbf{F}$	: Global force vector
$C$	: Structural compliance
$\mathbf{I}$	: Identity matrix

## References

- [1] A. G. Evans, J. W. Hutchinson and M. F. Ashby, Multifunctionality of cellular metal systems, *Progress in Materials Science*, 43 (3) (1998) 171-221.
- [2] M. P. Bendsøe and N. Kikuchi, Generating optimal topologies in structural design using a homogenization method, *Computer Methods in Applied Mechanics and Engineering*, 71 (2) (1988) 197-224.
- [3] M. P. Bendsøe, Optimal shape design as a material distribution problem, *Structural Optimization*, 1 (4) (1989) 193-202.
- [4] L. Xia, Q. Xia, X. Huang and Y. M. Xie, Bi-directional evolutionary structural optimization on advanced structures and materials: A comprehensive review, *Archives of Computational Methods in Engineering*, 25 (2) (2018) 437-478.
- [5] C. Lei, T. H. Baek and G. W. Jang, P1-Nonconforming shell element and its application to topology optimization, *Journal of Mechanical Science and Technology*, 29 (1) (2015) 297-308.
- [6] D. Lee and S. Shin, Extended-finite element method as analysis model for Gauss point density topology optimization method, *Journal of Mechanical Science and Technology*, 29 (4) (2015) 1341-1348.
- [7] J. Li, S. Chen and H. Huang, Topology optimization of continuum structure with dynamic constraints using mode identification, *Journal of Mechanical Science and Technology*, 29 (4) (2015) 1407-1412.
- [8] J. Hur, P. Kang and S. K. Youn, Topology optimization based on spline-based meshfree method using topological derivatives, *Journal of Mechanical Science and Technology*, 31 (5) (2017) 2423-2431.
- [9] S. M. Lee and S. Y. Han, Topology optimization based on the harmony search method, *Journal of Mechanical Science and Technology*, 31 (6) (2017) 2875-2882.
- [10] J. Du and R. Yang, Vibro-acoustic design of plate using bi-material microstructural topology optimization, *Journal of Mechanical Science and Technology*, 29 (4) (2015) 1413-1419.
- [11] A. Li, C. S. Liu and S. Z. Feng, Topology and thickness optimization of an indenter under stress and stiffness constraints, *Journal of Mechanical Science and Technology*, 32 (1) (2018) 211-222.
- [12] H. S. Park, T. T. Nguyen and P. Dahal, Development of a new concrete pipe molding machine using topology optimization, *Journal of Mechanical Science and Technology*, 30 (8) (2016) 3757-3765.
- [13] J. Zowe, M. Kočvara and M. P. Bendsøe, Free material optimization via mathematical programming, *Mathematical Programming*, 79 (1-3) (1997) 445-466.
- [14] L. Xia and P. Breitkopf, Concurrent topology optimization design of material and structure within FE<sup>2</sup> nonlinear multiscale analysis framework, *Computer Methods in Applied Mechanics and Engineering*, 278 (2014) 524-542.
- [15] P. G. Coelho, J. M. Guedes and H. C. Rodrigues, Multiscale topology optimization of bi-material laminated composite structures, *Composite Structures*, 132 (2015) 495-505.
- [16] L. Liu, J. Yan and G. Cheng, Optimum structure with homogeneous optimum truss-like material, *Computers & Structures*, 86 (13-14) (2008) 1417-1425.
- [17] R. Sivapuram, P. D. Dunning and H. A. Kim, Simultaneous material and structural optimization by multiscale topology optimization, *Structural and Multidisciplinary Optimization*, 54 (5) (2016) 1267-1281.
- [18] W. Chen, L. Tong and S. Liu, Concurrent topology design of structure and material using a two-scale topology optimization, *Computers & Structures*, 178 (2017) 119-128.
- [19] K. Long, X. Wang and X. Gu, Concurrent topology optimization for minimization of total mass considering load-carrying capabilities and thermal insulation simultaneously, *Acta Mechanica Sinica*, 34 (2) (2018) 315-326.
- [20] J. Deng and W. Chen, Concurrent topology optimization of multiscale structures with multiple porous materials under random field loading uncertainty, *Structural and Multidisciplinary Optimization*, 56 (1) (2017) 1:19.
- [21] J. Zhao, H. Yoon and B. D. Youn, An efficient decoupled sensitivity analysis method for multiscale concurrent topology optimization problems, *Structural and Multidisciplinary Optimization*, 58 (2) (2018) 445-457.
- [22] K. Svanberg, The method of moving asymptotes—a new method for structural optimization, *International Journal for Numerical Methods in Engineering*, 24 (2) (1987) 359-373.

- [23] Y. L. Mei, X. M. Wang and G. D. Cheng, Binary discrete method of topology optimization, *Applied Mathematics and Mechanics*, 28 (6) (2007) 707-719.
- [24] A. Ferrer, J. C. Cante, J. A. Hernández and J. Oliver, Two-scale topology optimization in computational material design: An integrated approach, *International Journal for Numerical Methods in Engineering*, 114 (3) (2018) 232-254.
- [25] O. Sigmund, Morphology-based black and white filters for topology optimization, *Structural and Multidisciplinary Optimization*, 33 (4-5) (2007) 401-424.



**Heting Qiao** (Corresponding author) received his B.S. degree from the Dalian University of Technology (2004) in Mechanical Engineering, and M.S. (2007) from Dalian University of technology and Ph.D.(2011) degrees, both in Engineering Mechanics. He has been a teacher at Shenyang University of technology since 2013. His interests include finite element method and structure optimization.  
E-mail: qiaoheting@mail.neu.edu.cn.